

Spatial distribution of environmental DNA in a nearshore marine habitat

James L. O'Donnell^{*1}, Ryan P. Kelly¹, Andrew O. Shelton², Jameal F. Samhouri², Natalie C. Lowell^{1,3}, and Gregory D. Williams⁴

¹School of Marine and Environmental Affairs, University of Washington, 3707 Brooklyn Ave NE, Seattle, Washington 98105, USA

²Northwest Fisheries Science Center, NOAA Fisheries, 2725 Montlake Blvd E, Seattle, Washington 98112, USA

³School of Aquatic and Fishery Sciences, University of Washington, 1122 NE Boat St, Seattle, Washington 98105, USA

⁴Pacific States Marine Fisheries Commission, Under contract to the Northwest Fisheries Science Center, NOAA Fisheries, 2725 Montlake Blvd E, Seattle, WA 98112

November 18, 2016

Keywords

metagenomics, metabarcoding, environmental monitoring, molecular ecology, marine, estuarine

^{*}jodonnellbio@gmail.com

Abstract

In the face of increasing threats to biodiversity, the advancement of methods for surveying biological communities is a major priority for ecologists. Recent advances in molecular biological technologies have made it possible to detect and sequence DNA from environmental samples (environmental DNA or eDNA); however, eDNA techniques have not yet seen widespread adoption as a routine method for biological surveillance primarily due to gaps in our understanding of the dynamics of eDNA in space and time. In order to identify the effective spatial scale of this approach in a dynamic marine environment, we collected marine surface water samples from transects ranging from the intertidal zone to 4 kilometers from shore. Using massively parallel sequencing of 16S amplicons, we identified a diverse community of metazoans and quantified their spatial patterns using a variety of statistical tools. We find evidence for multiple, discrete eDNA communities in this habitat, and show that these communities decrease in similarity as they become further apart. Offshore communities tend to be richer but less even than those inshore, though diversity was not spatially autocorrelated. Taxon-specific relative abundance coincided with our expectations of spatial distribution in taxa lacking a microscopic, pelagic life-history stage, though most of the taxa detected do not meet these criteria. Finally, we use carefully replicated laboratory procedures to show that laboratory treatments were remarkably similar in most cases, while allowing us to detect a faulty replicate, emphasizing the importance of replication to metabarcoding studies. While there is much work to be done before eDNA techniques can be confidently deployed as a standard method for ecological monitoring, this study serves as a first analysis of diversity at the fine spatial scales relevant to marine ecologists and confirms the promise of eDNA in dynamic environments.

Introduction

The patterns and causes of variability in ecological communities across space are both seminal and contentious areas of study in ecology (Hubbell, 2001; Anderson et al., 2011). One consistently observed pattern of community spatial heterogeneity is that communities close to one another tend to be more similar than those that are farther apart (Nekola and White, 1999). This decrease in community similarity with increasing spatial separation is called distance decay and has been reported from communities of tropical trees (Condit, 2002; Chust et al., 2006), ectomycorrhizal fungi

29 (Bahram et al., 2013), salt marsh plants (Guo et al., 2015), and microorganisms (Martiny et al.,
30 2011; Chust et al., 2013; Wetzel et al., 2012; Bell, 2010). Typically, this relationship is assessed by
31 regressing a measure of community similarity against a measure of spatial separation for a set of
32 sites at which a set of species' abundances (or presences) is calculated. Yet no existing biodiversity
33 survey method completely censuses all of the organisms in a given area. The lack of a single 'silver
34 bullet' method of sampling contributes inconclusiveness to the study of spatial patterning in ecology
35 (Levin, 1992), and leaves open the possibility of new and more comprehensive methods.

36 From a boat or aircraft, scientists can count whales by sight, but not the krill on which they
37 feed. For example, towed fishing nets can efficiently sample organisms larger than the mesh and
38 slower than the boat; but overlook viruses and have undesirable effects on charismatic air-breathing
39 species. However, DNA-based surveys show great promise as an efficient technique for detecting a
40 previously unthinkable breadth of organisms from a single sample.

41 Microbiologists have used nucleic acid sequencing to quantify the composition and function of
42 microbial communities in a wide variety of habitats (Handelsman et al., 1998; Tyson et al., 2004;
43 Venter et al., 2004; Iverson et al., 2012). To do so, a sample of environmental medium (e.g. water)
44 containing microorganisms is collected, their DNA or RNA is isolated and sequenced, and the
45 identity and abundance of sequences is considered to reflect the community of organisms contained
46 in the sample, which indirectly estimates the quantity of organisms in an area.

47 Macroorganisms shed DNA-containing cells into the environment (environmental DNA or eDNA)
48 that can be sampled in the same way (Ficetola et al., 2008; Thomsen et al., 2012). Potentially, eDNA
49 methods allow a broad swath of macroorganisms to be surveyed from basic environmental samples.
50 However, the accuracy and reliability of indirect estimates of macroorganismal abundance has been
51 debated because the entire organisms are not contained within the sample (Cowart et al., 2015).
52 Concern surrounding eDNA methods is rooted in uncertainty about the attributes of eDNA in the
53 environment relative to actual organisms (Shelton et al., 2016; Evans et al., 2016). Basic questions
54 such as how long DNA can persist in that environment and how far DNA can travel remain largely
55 unknown (but see Klymus et al. (2015); Turner et al. (2015); Strickler et al. (2015); Deiner and
56 Altermatt (2014)) and impede inference about local organismal presence from an environmental
57 sample. As a result, estimating the spatial and temporal resolution of eDNA studies in the field is
58 a key step in making these methods practical.

59 The relationship between local organismal abundance and eDNA is further complicated in habi-
60 tats where the environmental medium itself may transport eDNA away from its source. We know
61 that genetic material moves away from its source precisely because organisms can be detected indi-
62 rectly without being present in the sample (Kelly et al., 2016). One might reasonably expect eDNA
63 to travel farther in a highly dynamic fluid such as the open ocean or flowing river than it would
64 through the sediment at the bottom of a stagnant pond (Deiner and Altermatt, 2014; Shogren et al.,
65 2016). Yet even studies of extremely dynamic habitats such as coastlines with high wave energy
66 have found remarkable evidence that eDNA transport is limited enough that DNA methods can
67 detect differences among communities separated by less than 100 meters (Port et al., 2016).

68 While rigorous laboratory studies have investigated the effects of some environmental factors on
69 eDNA persistence (Klymus et al., 2015; Barnes et al., 2014; Sassoubre et al., 2016) and the transport
70 of eDNA in specific contexts (Deiner and Altermatt, 2014), we suggest that field studies comparing
71 the spatial distribution of communities of eDNA with expectations based on prior knowledge of
72 organisms' distributions are also critical to developing a working understanding of eDNA in the real
73 world.

74 We apply methods derived from community ecology to understand spatial patterns and patchi-
75 ness of eDNA. The underlying mechanism thought to drive the slope of the distance decay relation-
76 ship in ecological communities is the rate of movement of individuals among sites, which may be
77 driven by underlying processes such as habitat suitability. Because eDNA is shed and transported
78 away from its source, the increased movement of eDNA particles should homogenize community
79 similarity, and thus erode the distance decay relationship of eDNA communities.

80 Puget Sound is a deep, narrow fjord in Washington, USA, where a narrow band of shallow
81 bottom hugs the shoreline and abruptly gives way to a central depth of up to 300 meters. This
82 form allows the juxtaposition of communities associated with distinctly different habitats: shallow,
83 intertidal benthos, and euphotic pelagic (Burns, 1985). At the upper reaches of the intertidal, the
84 shoreline substrate varies from soft, fine sediment to cobble and boulder rubble. Soft intertidal
85 sediments are inhabited by burrowing bivalves (*Bivalvia*), segmented worms (*Annelida*), and acorn
86 worms (*Enteropneusta*), and in some lower intertidal and high subtidal ranges by eelgrass (*Zostera*
87 *marina*) (Kozloff, 1973; Dethier, 2010). Eelgrass meadows harbor epifaunal and infaunal biota,
88 and attract transient species which use the meadows for shelter and to feed on resident organisms.

89 Hard intertidal surfaces support a well-documented biota including barnacles (Sessilia), mussels
90 (Bivalvia:Mytilidae), anemones (Actinaria), sea stars (Asteroidea), urchins (Echinoidea), Bryzoans
91 (Ectoprocta), crustaceans (Decapoda), and a variety of algae (Dethier, 2010). Hard bottoms of the
92 lower intertidal and high subtidal are home to macroalgae such as Laminariales and Desmarestiales
93 which provides habitat for a distinct community of fish and invertebrates. The upper pelagic is
94 home to a diverse assemblage of microscopic plankton including diatoms and larvae (Strickland,
95 1983), as well as transitory fish and marine mammals.

96 We took advantage of this setting to explore the spatial variation and distribution of marine
97 eDNA communities. Using PCR-based methods and massively parallel sequencing, we surveyed
98 mitochondrial 16S sequences from a suite of marine animals in water samples collected over a grid
99 of sites extending from the shoreline out to 4 kilometers offshore in Puget Sound, Washington, USA.
100 We leverage this sampling design to perform the first explicitly spatial analysis of eDNA-derived
101 community similarity. We investigate two primary objectives. First we examine the spatial pattern-
102 ing of eDNA and determine the degree to which eDNA community similarity can be predicted by
103 physical proximity. We expect that physical proximity will be a strong predictor of community sim-
104 ilarity, and that community differences can be detected over small distances. Second, we examine
105 the distribution of diversity from eDNA data, and compare it to our expectations based on distri-
106 butions of macrobial communities. We expect that distinct eDNA communities exist in this setting,
107 and that their spatial distribution coincides with that of adult macrobial organisms. Because of the
108 vastly different communities of benthic macrobial metazoans as a function of distance from shore,
109 we expect that more than one eDNA community is present across our 4 kilometer sampling grid,
110 and that communities change as a function of distance from shore. For this reason, we examine two
111 diversity measures of eDNA communities that have been widely used to reveal broad scale patterns
112 based on macrobiota in many ecological systems. Finally, we identify the taxa represented in the
113 eDNA communities, which span a range of life-history characteristics, and we expect that the spatial
114 distribution of eDNA will most closely resemble the distribution of adults in taxa with low dispersal
115 potential.

116 **Methods**

117 There are seven discrete steps to our methodology: (1) Environmental sample collection, (2) isolation
118 of particulates from water via filtration, (3) isolation of DNA from filter membrane, (4) amplification
119 of target locus via PCR, (5) sequencing of amplicons, (6) bioinformatic translation of raw sequence
120 data into tables of sequence abundance among samples, and (7) community ecological analyses of
121 eDNA. We provide brief overviews of these steps here, and encourage the reader to review the fully
122 detailed methods presented in the supplementary material (Supplemental Material).

123 **Environmental Sampling**

124 Starting from lower-intertidal patches of *Zostera marina*, we collected water samples at 1 meter
125 depth from 8 points (0, 75, 125, 250, 500, 1000, 2000, and 4000 meters) along three parallel transects
126 separated by 1000 meters (24 sample locations total; Figure 1). To destroy residual DNA on
127 equipment used for field sampling and filtration, we washed with a 1:10 solution of household bleach
128 (8.25% sodium hypochlorite; 7.25% available chlorine) and deionized water, followed by thorough
129 rinsing with deionized water. Each environmental sample was collected in a clean 1 liter high-density
130 polyethylene bottle, the opening of which was covered with 500 micrometer nylon mesh to prevent
131 entry of larger particles. Immediately after collecting the sample, the mesh was replaced with a
132 clean lid and the sample was held on ice until filtering.

133 **Filtration**

134 One liter from each water sample was filtered in the lab on a clean polysulfone vacuum filter
135 holder fitted with a 47 millimeter diameter cellulose acetate membrane with 0.45 micrometer pores.
136 Filter membranes were moved into 900 microliters of Longmire buffer (Longmire et al., 1997) using
137 clean forceps and stored at room temperature (Renshaw et al., 2014). To test for the extent of
138 contamination attributable to laboratory procedures, we filtered three replicate 1 liter samples of
139 deionized water. These samples were treated identically to the environmental samples throughout
140 the remaining protocols.

141 DNA Purification

142 DNA was purified from the membrane following a phenol:chloroform:isoamyl alcohol protocol follow-
143 ing Renshaw (Renshaw et al., 2014). Preserved membranes were incubated at 65C for 30 minutes
144 before adding 900 microliters of phenol:chloroform:isoamyl alcohol and shaking vigorously for 60
145 seconds. We conducted two consecutive chloroform washes by centrifuging at 14,000 rpm for 5
146 minutes, transferring the aqueous layer to 700 microliters chloroform, and shaking vigorously for 60
147 seconds. After a third centrifugation, 500 microliters of the aqueous layer was transferred to tubes
148 containing 20 microliters 5 molar NaCl and 500 microliters 100% isopropanol, and frozen at -20C
149 for approximately 15 hours. Finally, all liquid was removed by centrifuging at 14000 rpm for 10
150 minutes, pouring off or pipetting out any remaining liquid, and drying in a vacuum centrifuge at
151 45C for 15 minutes. DNA was resuspended in 200 microliters of ultrapure water. Genomic DNA
152 extracted from tissue of a species absent from the sampled environment (*Oreochromis niloticus*)
153 served as positive control for the remaining protocols.

154 PCR Amplification

155 From each DNA sample, we amplified an approximately 115 base pair (bp) region of the mito-
156 chondrial gene encoding 16S RNA using a two-step polymerase chain reaction (PCR) protocol
157 described by O'Donnell et al. (2016). In the first set of reactions, primers were identical in ev-
158 ery reaction (forward: AGTTACYYTAGGGATAACAGCG; reverse: CCGGTCTGAACTCAGAT-
159 CAYGT); primers in the second set of reactions included these same sequences but with 3 variable
160 nucleotides (NNN) and an index sequence on the 5' end (see Sequencing Metadata). We used the
161 program OligoTag (Coissac, 2012) to generate 30 unique 6-nucleotide index sequences differing by
162 a minimum Hamming distance of 3 (see Sequencing Metadata). Indexed primers were assigned to
163 samples randomly, with the identical index sequence on the forward and reverse primer to avoid
164 errors associated with dual-indexed multiplexing (Schnell et al., 2015). In a UV-sterilized hood,
165 we prepared 25 microliter reactions containing 18.375 microliters ultrapure water, 2.5 microliters
166 10x buffer, 0.625 microliters deoxynucleotide solution (8 millimolar), 1 microliter each forward and
167 reverse primer (10 micromolar, obtained lyophilized from Integrated DNA Technologies (Coralville,
168 IA, USA)), 0.25 microliters Qiagen HotStar Taq polymerase, and 1.25 microliter genomic eDNA

169 template at 1:100 dilution in ultrapure water. PCR thermal profiles began with an initialization
170 step (95C; 15 min) followed by cycles (40 and 20 for the first and second reaction, respectively) of
171 denaturation (95C; 15 sec), annealing (61C; 30 sec), and extension (72C; 30 sec). 20 identical PCRs
172 were conducted from each DNA extract using non-indexed primers; these were pooled into 4 groups
173 of 5 in order to ensure ample template for the subsequent PCR with indexed primers. In order to
174 isolate the fragment of interest from primer dimer and other spurious fragments generated in the
175 first PCR, we used the AxyPrep Mag FragmentSelect-I kit with solid-phase reversible immobiliza-
176 tion (SPRI) paramagnetic beads at 2.5x the volume of PCR product (Axygen BioSciences, Corning,
177 NY, USA). A 1:5 dilution in ultrapure water of the product was used as template for the second
178 reaction. PCR products of the second reaction were purified using the Qiagen MinElute PCR Pu-
179 rification Kit (Qiagen, Hilden, Germany). Ultrapure water was used in place of template DNA and
180 run along with each batch of PCRs to serve as a negative control for PCR; none of these produced
181 visible bands on an agarose gel. In total, four separate replicates from each of 31 DNA samples
182 were carried through the two-step PCR process for a total of 124 sequenced PCR products. These
183 were combined with additional samples from other projects, totaling 345 samples for sequencing.

184 **DNA Sequencing**

185 PCR products were pooled according to their primer index in equal concentration, and 150 ng was
186 prepared for library sequencing using the KAPA high-throughput library prep kit with real-time
187 library amplification protocol (KAPA Biosystems, Wilmington, MA, USA). Each of these ligated
188 sequencing adapter including an additional 6 base pair index sequence (NEXTflex DNA barcodes;
189 BIOO Scientific, Austin, TX, USA). Thus, each PCR product was identifiable via its unique com-
190 bination of index sequences in the sequencing adapters and primers. Fragment size distribution
191 and concentration of each library was quantified using an Agilent 2100 BioAnalyzer. Libraries were
192 pooled in equal concentrations and sequenced for 150 base pairs in both directions (PE150) using
193 an Illumina NextSeq at the Stanford Functional Genomics Facility (machine NS500615, run 115,
194 flowcell H3LFLAFX), where 20% PhiX Control v3 was added to act as a sequencing control and
195 to enhance sequencing depth. Raw sequence data in fastq format is publicly available (see Data
196 Availability).

197 **Sequence Data Processing (Bioinformatics)**

198 Detailed bioinformatic methods are provided in the supplemental material, and analysis scripts
199 used from raw sequencer output onward can be found in the public project directory (see Analysis
200 Scripts). Briefly, we performed five steps to process the sequence data: (1) Merge paired-end
201 reads, (2) eliminate low-quality reads, (3) eliminate PCR artifacts (chimeras), (4) cluster reads by
202 similarity into operational taxonomic units (OTUs), and (5) match observed sequences to taxon
203 names. Additionally, we checked for consistency among PCR replicates, excluded extremely rare
204 sequences, and rescaled (rarefied) the data to account for differences in sequencing depth. The data
205 for input to further analyses are a contingency table of the mean count of unique sequences, OTUs,
206 or taxa present in each environmental sample.

207 **Ecological Analyses**

208 After gathering the data, we use the eDNA community observed at each location to make inferences
209 about the spatial patterning of eDNA communities. We use statistical tools from community ecology
210 to assess the spatial structure of eDNA communities. We report similarity (1- dissimilarity) rather
211 than dissimilarity in all cases for ease of interpretation.

212 **Objective 1: Community similarity as a function of distance**

213 **Distance Decay**

214 To address our first objective and determine whether or not nearby samples are more similar than
215 distant ones, we fit a nonlinear model to represent decreasing community similarity with distance.
216 We calculated the pairwise Bray-Curtis similarity (1 - Bray-Curtis dissimilarity) between eDNA
217 communities using the R package *vegan* (Oksanen et al., 2016) and the great circle distance between
218 sampling points using the Haversine method as implemented by the R package *geosphere* (Hijmans,
219 2016). This model is similar to the Michaelis-Menten function, but with an asymptote fixed at 0:

$$y_{ij} = \frac{AB}{B + x_{ij}} \quad (1)$$

220 Where the relationship between community similarity (y_{ij}) and spatial distance (x_{ij}) between

221 observations i and j is determined by the similarity of samples at distance 0 (A), and the distance at
 222 which half the total change in similarity is achieved (B). This allows for a samples collected very close
 223 together (near 0) to have similarity significantly less than one. We assessed model fit using the R
 224 function `nls` (R Core Team, 2016), using the `nl2sol` algorithm from the `Port` library to solve separable
 225 nonlinear least squares using analytically computed derivatives (<http://netlib.org/port/nsg.f>). We
 226 set bounds of 0 and 1 for the intercept parameter and a lower bound of 0 for the distance at half
 227 similarity; starting values of these parameters were 0.5 and $x_{max}/2$, respectively. We calculated
 228 a 95% confidence interval for the parameters and the predicted values using a first-order Taylor
 229 expansion approach implemented by the function `predictNLS` in the R package `propagate` (Spiess,
 230 2014).

231 There are other conceptually reasonable forms to expect the space-by-similarity relationship
 232 to take; we present these in the supplemental material along with alternative data subsets and
 233 similarity indices (see Supplemental Material).

234 **Objective 2: Spatial distribution of diversity**

235 **Community Classification**

236 To determine the spatial distribution and variation of eDNA communities (objective 2), we used
 237 multivariate classification algorithms. We simultaneously assessed the existence of distinct com-
 238 munity types and the membership of samples to those community types using an unsupervised
 239 classification algorithm known as partitioning around medoids (PAM; sometimes referred to as k-
 240 medoids clustering) (Kaufman and Rousseeuw, 1990), as implemented in the R package `cluster`
 241 (Maechler et al., 2016). The classification of samples to communities was made on the basis of
 242 their pairwise Bray-Curtis similarity, calculated using the function `vegdist` in the R package `vegan`
 243 (Oksanen et al., 2016). Other distance metrics were evaluated but had no appreciable effect on the
 244 outcome of the analysis (Figure 8). In order to chose an optimal number of clusters (K), we evalu-
 245 ated the distribution of silhouette widths, a measure of the similarity between each sample and its
 246 cluster compared to its similarity to other clusters. We repeated the analysis using fuzzy clustering
 247 (FANNY, (Kaufman and Rousseeuw, 1990); however, the results were qualitatively similar to the
 248 results using PAM so we omit them here.

249 **Aggregate Measures of Diversity**

250 We calculated two measures of diversity, richness and evenness, to ask if aggregate metrics of the
251 eDNA community showed evidence of spatial patterning. Richness is a measure of the number of
252 distinct types of organisms present and so ranges from 1 (only one taxon observed) to S , the number
253 of taxa observed across all samples. To calculate the evenness of the distribution of abundance of
254 taxa in a sample, we used the complement of the Simpson (1949) index ($1 - \sum p_i^2$, where p_i is the
255 proportional abundance of taxon i). The values of this index ranges from 0 to 1, with the value
256 interpreted as the probability that two sequences randomly selected from the sample will belong to
257 different taxa; thus, larger values of the index indicate more evenly divided communities (Magurran,
258 2003). We calculated Moran's I for both diversity metrics to test for spatial autocorrelation. We
259 also tested for a linear effect of log-transformed distance from shore on each measure of diversity to
260 ask how diversity changes over this strong environmental gradient.

261 **Taxon and Life History Patterns**

262 After assigning taxon names to the abundance data, we plotted the distribution in space of a
263 selection of taxa to compare with our expectations on the basis of adult distributions (objective 2).
264 Our aim was to understand where each taxon occurred in the greatest proportional abundance, and
265 its distribution in space relative to that maximum. Thus, we rescaled each sample to proportional
266 abundance, extracted the data from a single taxon, and scaled those values between 0 and 1.
267 We collated life history characteristics for each of the major taxonomic groups recovered, including
268 dispersal range of the gametes, larvae, and adults, adult habitat type and selectivity, and adult body
269 size. Dispersal range was given as an order-of-magnitude approximation of the scale of dispersal:
270 for example, internally fertilized species were assigned a gamete range of 0 km, while broadcast
271 spawners were assigned a gamete range of 10 km. Similarly, adult range size was approximated as
272 0 km (sessile), 1 km (motile but not pelagic), or 10 km (highly mobile, pelagic). Variables were
273 specified as 'multiple' for groups known to span more than 1 magnitude of range size. For groups to
274 which sequences were annotated with high confidence, but for which life history strategy is diverse or
275 poorly known (e.g. families in the phylum Nemertea), we used conservative, coarse approximations
276 at a higher taxonomic rank (see Life History Data).

277 **Results**

278 **Sequence Data Processing (Bioinformatics)**

279 Preliminary sequence analysis strongly suggested that the observed variation among environmental
280 samples reflects true variation in the environment, rather than variability due to lab protocols, for
281 the following reasons (note that all value ranges are reported as mean plus and minus one standard
282 deviation). First, all libraries passed the FastQC per-base sequence quality filter, generating a total
283 of 371,576,190 reads passing filter generated in each direction. Second, samples in this study were
284 represented by an adequate number of reads ($333,537.9 \pm 112,200.5$), with no individual sample
285 receiving fewer than 130,402 reads. Third, there was a very low frequency of cross-contamination
286 from other libraries into those reported here ($5e-05 \pm 8e-05$; max proportion 0.00034). Fourth, after
287 scaling all samples to the same sequencing depth, OTUs with abundance greater than 178 reads
288 (0.14% of a sample's reads) experienced no turnover among PCR replicates within a sample. Fifth,
289 sequence abundances among PCR replicates within water samples were remarkably consistent. A
290 single sample had low similarity among PCR replicates (0.659) after removing this outlier, the
291 lowest mean similarity among replicates within a sample was 0.966. Overall similarities among
292 PCR replicates within a sample were extremely high (0.976 ± 0.013), and far higher than that of
293 than among samples (0.3 ± 0.16).

294 **Ecological Analyses**

295 **Distance Decay**

296 Physical proximity is a good predictor of eDNA community similarity: Similarity decreased from
297 0.40 (95%CI = 0.36, 0.45) to half that amount at 4500 meters (95%CI = 2900, 7500) (Figure 2).

298 **Community Classification**

299 Despite a clear trend in community similarity as a function of spatial separation, the results from
300 our classification analysis are difficult to interpret. The silhouette analysis indicated the presence
301 of 8 distinct communities; however, the gain in mean silhouette width from 2 was small (0.1), and
302 lacked a distinctive peak (Figure 4), indicating substantial uncertainty in the clustering algorithm.

Thus, we present the results of cluster assignment for both $K = 2$ and $K = 8$ to illustrate the range of results (Figure 3). Excluding taxa which occur in only one site had no discernible effect on the outcome of the PAM analysis (number of clusters, assignment to clusters). While there was no distinct spatial divide indicating the presence of an inshore versus an offshore community, one of the two communities (at $K = 2$) occurred in only 2 out of 18 samples inside 1000 meters from shore, and never occurred within 125 meters of shore, suggesting the presence of an inshore and offshore community.

Diversity in Space

Sites offshore tend to be less rich and more even than those inshore (Figure 6). Mean OTU richness declined by 1.42 per 1000 meters from a mean of 17.6 taxa (95%CI = 2.15) inshore to 11.9 taxa (95%CI = 4.31) at offshore locations ($p = 0.0415$; Figure 6). Evenness, the probability that two reads chosen at random from a sample belong to different species, increased by .0666 per 1000 meters from 0.225 (95%CI = 0.0558) to 0.491 (95%CI = ± 0.112), indicating that sequence reads were less evenly distributed among taxa in offshore samples ($p \ll 0.05$; Figure 6). There was no evidence for spatial autocorrelation for any of the diversity metrics (Moran's I, $p > 0.05$; Figure 5).

Taxon and Life History Patterns

We were able to assign a taxon name with confidence to 136 of 146 OTU sequences. The vast majority of sequences (97.6%) and OTUs (96.9%) were matched to organisms that have high potential for dispersal at either the gamete, larval, or adult stage, making it impossible to determine whether the source of that DNA was adults with well-documented spatial patterns (e.g. sessile nearshore specialists) or highly mobile early life history stages. Of the 6 OTUs for which dispersal is limited during all life history stages, only 2 occurred in more than two samples, precluding a quantitative comparison of spatial dispersion based on life history characteristics. These were assigned to *Cymatogaster aggregata*, a viviparous nearshore fish with internal fertilization, and *Cupolaconcha meroclista*, a sessile Vermetid gastropod with presumed internal fertilization and short larval dispersal (Strathmann and Strathmann, 2006; Phillips and Shima, 2010; Calvo and Templado, 2004). *Cymatogaster aggregata* was distinctly more abundant close to shore, with no sequences occurring in any sample beyond 250 meters (Figure 7). *Cupolaconcha meroclista* showed no such distinct spatial

331 trend, occurring in nearly equal abundance at three sites, 75, 500, and 2000 meters from shore. An
332 additional species that was highly abundant in the sequence data, the krill *Thysanoessa raschii*,
333 has pelagic adults, highly seasonal reproduction, and sinking eggs; their distribution was consistent
334 with our expectations based on a tendency of adults to aggregate offshore. Finally, the two most
335 abundant taxa in the dataset were the mussel genus *Mytilus* and the Barnacle order Sessilia; the
336 adults of both taxa are sessile and occur exclusively on hard intertidal substrata but have highly
337 motile larvae.

338 Discussion

339 Indirect surveys of organismal presence are a key development in ecosystem monitoring in the face
340 of increased anthropogenic pressure and dwindling resources for ecological research. Monitoring
341 of organisms using environmental DNA is an especially promising method, given the rapid pace
342 of advancement in technological innovation and cost efficiency in the field of DNA sequencing and
343 quantification. For the first time in a marine environment, we document four key patterns: (1) eDNA
344 communities far from one another tend to be less similar than those that are nearby, (2) distinct
345 eDNA communities exist and are distributed in a non-random fashion, (3) diversity declines with
346 distance from shore, and (4) spatial patterning of eDNA is associated with taxon-specific life history
347 characteristics.

348 (1) Communities far from one another tend to be less similar than those that are 349 nearby

350 We demonstrate that more distant locations have less similar eDNA communities than more proxi-
351 mate locations in Puget Sound, a dynamic marine environment. Our finding is in line with observa-
352 tions based on traditional surveys of terrestrial plants and fungi (Nekola and White, 1999; Bahram
353 et al., 2013; Condit, 2002; Chust et al., 2006) and of microorganisms in freshwater (Wetzel et al.,
354 2012), marine (Chust et al., 2013), and estuarine (Martiny et al., 2011) environments. To our knowl-
355 edge, it is the first to report such a pattern using massively parallel sequencing of environmental
356 DNA in the marine environment, and the first using any technique to describe this pattern from
357 microbial metazoans. We note that the theoretical expectation is that samples at very close distance

358 be nearly completely similar, while our samples separated by the 50 meters were only 40% similar.
359 We interpret this to reflect the highly dynamic nature of this environment, which could cause DNA
360 to be distributed quickly from its source, eroding the rise in similarity at small distances. At the
361 same time, community similarity decreased to very low levels at larger scales, indicating that DNA
362 distribution is not completely unpredictable. This finding implies that the effectively sampled area
363 of individual water samples for eDNA analysis is likely to be quite small ($<100\text{m}$) in this nearshore
364 environment. Our estimated distance-decay relationship does indicate that proximate samples are
365 more similar than distant samples, but we suggest this pattern is partially obscured by other factors,
366 including signal from mobile, microscopic life-stages.

367 **(2) Distinct eDNA communities exist and are distributed in a non-random fashion**

368 We demonstrate strong evidence for distinct community types and the non-random spatial pattern-
369 ing of those communities. While the spatial distributions of communities is surprising if one were
370 concerned only with the macroscopic life stages of metazoans, it indeed does align with the broader
371 view that even offshore pelagic communities are comprised of and influenced by nearshore organ-
372 isms. This result underscores the idea that areas immediately offshore act as ecotones, a mixing
373 zone of taxa characteristic of benthic and pelagic environments. While there was no distinct break
374 in community types between onshore and offshore sites, there was some clustering of community
375 types that may be explained by oceanographic features such as nearshore eddies generated by strong
376 tidal exchange in a steep bathymetric setting (Yang and Khangaonkar, 2010). It would be useful to
377 better understand such features during the period of sampling, by way of oceanographic monitoring
378 devices.

379 **(3) Richness declines and evenness increases with distance from shore**

380 We detected a general pattern of declining richness and increasing evenness with increasing distance
381 offshore. Such a pattern is consistent with many other ecosystems which show strong clines in
382 diversity metrics over environmental gradients. The coastal ocean is a highly productive and diverse
383 ecosystem (Ray, 1988). However, our study is novel in that it corroborates a cline well-known on
384 macroscales for macrobiota on a much smaller spatial scale for microscopic animals, suggesting that
385 there may be a self-similarity across scales in diversity patterning (Levin, 1992). Intriguingly, the

cline in diversity from inshore to offshore was not determined by shared changes in communities as one moved offshore; the classification analysis suggested a fair amount of differences among communities at a given offshore distance (Figure 3). Furthermore, the uncertainty in identification of the number of distinct clusters to best characterize the community underlines the difficulty of identifying community patterns with the number of taxonomic groups considered here. We suspect that the signature of eDNA from microscopic life-stages may explain our inability to easily detect spatial community level patterns that align with our initial expectations.

(4) Spatial patterning of eDNA is associated with taxon-specific life history characteristics.

In contrast to our expectations, other taxa including species with sessile adult stages restricted to benthic hard substrates (e.g. barnacles, mussels) are among the most abundant taxa at sites furthest from shore. However, the larvae and gametes of these taxa are abundant, pelagic, and can be transported long distances by water movement (Strathmann, 1987). This indicates that we likely detected DNA of their pelagic phase gametes and larvae. It is always possible that DNA of adults was advected over long distances and detected offshore but in light of our results with krill and surfperch, we view this as unlikely. We interpret our results as evidence that the chaotic spatial distribution of eDNA communities (Figure 3) results from our primers' affinity for many species which at some point exist as microscopic pelagic gametes or larvae. Our results emphasize that expected results based on easily visually observed individuals or detectable with traditional sampling gear such as nets may be very different from results using eDNA. This does caution that eDNA surveys may have different purposes and may not be directly comparable to existing surveys (Shelton et al., 2016).

We acknowledge that sampling artifacts may have affected our results. For example if entire multicellular individuals were captured in our samples, their DNA could be in much greater density than eDNA, affecting the observed community. Our sampling bottles excluded particles larger than 500 micrometers, but gametes and very small larvae could have gained entry. It is possible that even a single small individual, containing many thousand mitochondria, would overwhelm the signal of another species from which hundreds of cells had been sloughed from many, larger individuals. Data on larval size distribution at the time of sampling from each species in our data set would

415 allow us to estimate the frequency of such events. Nevertheless, it is precisely the sensitivity to
416 small particles that makes the eDNA approach powerful, so we are reluctant to recommend that
417 aquatic eDNA sampling use finer pre-filtering. Instead, we emphasize the importance of designing
418 and selecting primer sets that selectively amplify target organisms. In the case of the present study,
419 in order to recover patterns matching our expectations, this would be non-transient, benthic marine
420 organisms lacking any pelagic life stage.

421 Our results also highlight the need for curated life-history databases. As technological advances
422 increase the speed and throughput of DNA sequencing and sequence processing, making sense of
423 these data in a timely manner requires that natural history data be stored in standard formats in
424 centralized repositories. The rate at which we can make sense of high-throughput survey methods
425 will be limited by our ability to collate auxiliary data. Databases such as Global Biodiversity
426 Information Facility (GBIF), Encyclopedia of Life (EOL), and FishBase (Parr et al., 2014; Froese
427 and Pauly, 2016) contain records of taxonomy, occurrence, and other rudimentary data types, but
428 there is no centralized, standardized repository for even basic natural history data such as body
429 size. As NCBI's nucleotide and protein sequence database (GenBank) has facilitated a multitude of
430 transformative studies in diverse fields, an ecological analog would be a huge boon for biodiversity
431 science.

432 Surveys based on eDNA are intensely scrutinized because of the danger that the final data are
433 subject to complicated laboratory and bioinformatic procedures. Finding virtually no variability
434 among lab and bioinformatic treatments from the point of PCR onward, we were confident our
435 results represented actual field-based differences among samples. However, we note that one PCR
436 replicate had a clear signal of contamination in that the sequence community was extremely similar
437 to those from a different environmental sample. The source of this error is difficult to identify, but
438 seems most likely to be an error during PCR preparation, either in assignment or pipetting during
439 preparation of indexed primers. While the remainder of our results would be largely unchanged
440 had we sequenced a single replicate per environmental sample, we believe the sequencing of PCR
441 replicates is critical for ensuring data quality in eDNA sequencing studies.

442 While there is much work to be done before eDNA techniques can be confidently deployed as a
443 standard method for ecological monitoring, this study serves as a first analysis of diversity at the
444 fine spatial scales that are likely to be relevant to eDNA work in the field across a range of study

445 systems.

446 **Acknowledgements**

447 We wish to thank Robert Morris, E. Virginia Armbrust, and James Kralj.

448 **Funding**

449 This work was supported by a grant from the David and Lucile Packard Foundation to RPK (grant
450 2014-39827). The funders had no role in study design, data collection and analysis, decision to
451 publish, or preparation of the manuscript.

452 **Author Contributions**

453 Conceived and designed the experiments: JL O'Donnell, RP Kelly, AO Shelton; Collected the data:
454 JL O'Donnell, NC Lowell, GD Williams, RP Kelly, AO Shelton, JF Samhouri; Conducted the
455 analyses: JL O'Donnell; Wrote the first draft: JL O'Donnell; Edited the manuscript: JL O'Donnell,
456 AO Shelton, RP Kelly, JF Samhouri, GD Williams, NC Lowell

457 **Ethics Statement**

458 The authors declare no conflict of interest. No permits were required to do any of the research
459 described here.

460 **Data Availability**

461 **0.1 Sequence Data**

462 All sequence files and metadata are available from EMBL:

463 <http://www.ebi.ac.uk/ena/data/view/FIXME>

464 0.2 Project Repository

465 The following components are available from the project repository on GitHub:

466 https://github.com/jimmyodonnell/Carkeek_eDNA_grid

467 <http://dx.doi.org/FIXME>

468 0.2.1 Sequencing Metadata

469 Sequencing metadata is available in: `Data/metadata_spatial.csv`

470 0.2.2 Life History Data

471 Life history data is available in: `Data/life_history.csv`

472 0.2.3 Analysis Scripts

473 All analyses were performed using scripts available in the Analysis subdirectory.

474 References

475 Anderson, M. J., Crist, T. O., Chase, J. M., Vellend, M., Inouye, B. D., Freestone, A. L., Sanders,
476 N. J., Cornell, H. V., Comita, L. S., Davies, K. F., Harrison, S. P., Kraft, N. J. B., Stegen, J. C.,
477 and Swenson, N. G. (2011). Navigating the multiple meanings of beta diversity: A roadmap for
478 the practicing ecologist. *Ecology Letters*, 14(1):19–28.

479 Bahram, M., Kõljalg, U., Courty, P. E., Diédhiou, A. G., Kjølner, R., Pölme, S., Ryberg, M., Veldre,
480 V., and Tedersoo, L. (2013). The distance decay of similarity in communities of ectomycorrhizal
481 fungi in different ecosystems and scales. *Journal of Ecology*, 101(5):1335–1344.

482 Barnes, M. A., Turner, C. R., Jerde, C. L., Renshaw, M. A., Chadderton, W. L., and Lodge, D. M.
483 (2014). Environmental conditions influence eDNA persistence in aquatic systems. *Environmental*
484 *Science and Technology*, 48(3):1819–1827.

485 Bell, T. (2010). Experimental tests of the bacterial distance–decay relationship. *The ISME Journal*,
486 4(11):1357–1365.

487 Burns, R. E. (1985). *The shape and form of Puget Sound*. Washington Sea Grant, Seattle, 1 edition.

488 Calvo, M. and Templado, J. (2004). Reproduction and development in a vermetid gastropod,
489 *Vermetus triquetrus*. *Invertebrate Biology*, 123(4):289–303.

490 Camacho, C., Coulouris, G., Avagyan, V., Ma, N., Papadopoulos, J., Bealer, K., and Madden, T. L.
491 (2009). BLAST+: architecture and applications. *BMC Bioinformatics*, 10:421.

492 Chamberlain, S. a. and Szöcs, E. (2013). taxize: taxonomic search and retrieval in R. *F1000Research*,
493 2(0):191.

494 Chamberlain, S. A., Szöcs, E., Boettiger, C., Ram, K., Bartomeus, I., Foster, Z., and O’Donnell,
495 J. L. (2016). taxize: Taxonomic information from around the web. R package.

496 Chust, G., Chave, J., Condit, R., Aguilar, S., Lao, S., and Perez, R. (2006). Determinants and
497 spatial modeling of tree beta-diversity in a tropical forest landscape in Panama. *Journal of*
498 *Vegetation Science*, 17(1):83–92.

499 Chust, G., Irigoien, X., Chave, J., and Harris, R. P. (2013). Latitudinal phytoplankton distribution
500 and the neutral theory of biodiversity. *Global Ecology and Biogeography*, 22(5):531–543.

501 Coissac, E. (2012). OligoTag: A Program for Designing Sets of Tags for Next-Generation Sequencing
502 of Multiplexed Samples. In Pompanon, F. and Bonin, A., editors, *Data Production and Analysis in*
503 *Population Genomics SE - 2*, volume 888 of *Methods in Molecular Biology*, pages 13–31. Humana
504 Press.

505 Condit, R. (2002). Beta-Diversity in Tropical Forest Trees. *Science*, 295(5555):666–669.

506 Cowart, D. a., Pinheiro, M., Mouchel, O., Maguer, M., Grall, J., Miné, J., and Arnaud-Haond, S.
507 (2015). Metabarcoding Is Powerful yet Still Blind: A Comparative Analysis of Morphological and
508 Molecular Surveys of Seagrass Communities. *Plos One*, 10(2):e0117562.

509 Deiner, K. and Altermatt, F. (2014). Transport distance of invertebrate environmental DNA in a
510 natural river. *PLoS ONE*, 9(2).

511 Dethier, M. N. (2010). Overview of the ecology of Puget Sound beaches. In Shipman, H., Dethier,
 512 M. N., Gelfenbaum, G., Fresh, K. L., and Dinicola, R. S., editors, *Puget Sound Shorelines and*
 513 *the Impacts of Armoring—Proceedings of a State of the Science Workshop*, page 262.

514 Edgar, R. C. (2010). Search and clustering orders of magnitude faster than BLAST. *Bioinformatics*,
 515 26(19):2460–2461.

516 Evans, N. T., Olds, B. P., Renshaw, M. A., Turner, C. R., Li, Y., Jerde, C. L., Mahon, A. R.,
 517 Pfrender, M. E., Lamberti, G. A., and Lodge, D. M. (2016). Quantification of mesocosm fish and
 518 amphibian species diversity via environmental DNA metabarcoding. *Molecular Ecology Resources*,
 519 16(1):29–41.

520 Ficetola, G. F., Miaud, C., Pompanon, F., and Taberlet, P. (2008). Species detection using envi-
 521 ronmental DNA from water samples. *Biology letters*, 4(4):423–425.

522 Froese, R. and Pauly, D. (2016). FishBase.

523 Guo, H., Chamberlain, S. A., Elhaik, E., Jalli, I., Lynes, A. R., Marczak, L., Sabath, N., Vargas,
 524 A., Więski, K., Zelig, E. M., and Pennings, S. C. (2015). Geographic variation in plant commu-
 525 nity structure of salt marshes: Species, functional and phylogenetic perspectives. *PLoS ONE*,
 526 10(5):e0127781.

527 Handelsman, J., Rondon, M. R., Brady, S. F., Clardy, J., and Goodman, R. M. (1998). Molecular
 528 biological access to the chemistry of unknown soil microbes: a new frontier for natural products.
 529 *Chemistry & Biology*, 5(10):R245–R249.

530 Hijmans, R. J. (2016). *geosphere: Spherical Trigonometry*.

531 Hubbell, S. (2001). *The Unified Neutral Theory of Biodiversity and Biogeography.*, volume 32.

532 Iverson, V., Morris, R. M., Frazar, C. D., Berthiaume, C. T., Morales, R. L., and Armbrust,
 533 E. V. (2012). Untangling Genomes from Metagenomes: Revealing an Uncultured Class of Marine
 534 Euryarchaeota. *Science*, 335(6068):587–590.

535 Kaufman, L. and Rousseeuw, P. J. (1990). *Finding Groups in Data: An Introduction to Cluster*
 536 *Analysis*.

537 Kelly, R. P., O'Donnell, J. L., Lowell, N. C., Shelton, A. O., Samhour, J. F., Hennessey, S. M.,
 538 Feist, B. E., and Williams, G. D. (2016). Genetic signatures of ecological diversity along an
 539 urbanization gradient. *PeerJ*, 4:e2444.

540 Klymus, K. E., Richter, C. A., Chapman, D. C., and Paukert, C. (2015). Quantification of eDNA
 541 shedding rates from invasive bighead carp *Hypophthalmichthys nobilis* and silver carp *Hypoph-*
 542 *thalmichthys molitrix*. *Biological Conservation*, 183:77–84.

543 Kozloff, E. N. (1973). *Seashore life of Puget Sound, the Strait of Georgia, and the San Juan*
 544 *Archipelago*. University of Washington Press, Seattle.

545 Levin, S. A. (1992). The problem of pattern and scale in ecology. *Ecology*, 73(6):1943–1967.

546 Longmire, J. L., Maltbie, M., and Baker, R. J. (1997). Use of lysis buffer in DNA isolation and its
 547 implication for museum collections. *Museum of Texas Tech University*, 163.

548 Maechler, M., Rousseeuw, P., Struyf, A., Hubert, M., and Hornik, K. (2016). *cluster: Cluster*
 549 *Analysis Basics and Extensions*.

550 Magurran, A. E. (2003). *Measuring Biological Diversity*. Wiley.

551 Mahé, F., Rognes, T., Quince, C., de Vargas, C., and Dunthorn, M. (2014). Swarm: robust and
 552 fast clustering method for amplicon-based studies. *PeerJ*, 2:e593.

553 Martin, M. (2011). Cutadapt removes adapter sequences from high-throughput sequencing reads.
 554 *EMBnet.journal*, 17(1):10.

555 Martiny, J. B. H., Eisen, J. A., Penn, K., Allison, S. D., and Horner-Devine, M. C. (2011). Drivers of
 556 bacterial beta diversity depend on spatial scale. *Proceedings of the National Academy of Sciences*,
 557 108(19):7850–7854.

558 Nekola, J. C. and White, P. S. (1999). The distance decay of similarity in biogeography and ecology.
 559 *Journal of Biogeography*, 26(4):867–878.

560 O'Donnell, J. L., Kelly, R. P., Lowell, N. C., and Port, J. A. (2016). Indexed PCR Primers Induce
 561 Template-Specific Bias in Large-Scale DNA Sequencing Studies. *PLoS ONE*, 11(3):1–11.

562 Oksanen, J., Blanchet, F. G., Friendly, M., Kindt, R., Legendre, P., McGlinn, D., Minchin, P. R.,
 563 O'Hara, R. B., Simpson, G. L., Solymos, P., Stevens, M. H. H., Szoecs, E., and Wagner, H.
 564 (2016). *vegan: Community Ecology Package*.

565 Parr, C. S., Wilson, N., Leary, P., Schulz, K. S., Lans, K., Walley, L., Hammock, J. A., Goddard,
 566 A., Rice, J., Studer, M., Holmes, J. T. G., and Corrigan, R. J. (2014). The Encyclopedia of
 567 Life v2: Providing Global Access to Knowledge About Life on Earth. *Biodiversity Data Journal*,
 568 2(2):e1079.

569 Phillips, N. E. and Shima, J. S. (2010). Reproduction of the vermetid gastropod *dendropoma*
 570 *maximum* (Sowerby, 1825) in Moorea, French Polynesia. *Journal of Molluscan Studies*, 76(2):133–
 571 137.

572 Port, J. A., O'Donnell, J. L., Romero-Maraccini, O. C., Leary, P. R., Litvin, S. Y., Nickols, K. J.,
 573 Yamahara, K. M., and Kelly, R. P. (2016). Assessing vertebrate biodiversity in a kelp forest
 574 ecosystem using environmental DNA. *Molecular Ecology*, 25(2):527–541.

575 R Core Team (2016). *R: A Language and Environment for Statistical Computing*. R Foundation
 576 for Statistical Computing, Vienna, Austria.

577 Ray, G. C. (1988). Ecological diversity in coastal zones and oceans. In Wilson, E. O. and Peter,
 578 F. M., editors, *Biodiversity*, chapter 4. National Academies Press (US), Washington, DC.

579 Renshaw, M. A., Olds, B. P., Jerde, C. L., Mcveigh, M. M., and Lodge, D. M. (2014). The room
 580 temperature preservation of filtered environmental DNA samples and assimilation into a phenol-
 581 chloroform-isoamyl alcohol DNA extraction. *Molecular Ecology Resources*.

582 Rognes, T., Flouri, T., Nichols, B., Quince, C., and Mahé, F. (2016). VSEARCH: a versatile open
 583 source tool for metagenomics. *PeerJ*, 4:e2584.

584 Sassoubre, L. M., Yamahara, K. M., Gardner, L. D., Block, B. A., and Boehm, A. B. (2016).
 585 Quantification of Environmental DNA (eDNA) Shedding and Decay Rates for Three Marine
 586 Fish. *Environmental Science & Technology*, 50(19):10456–10464.

587 Schnell, I. B., Bohmann, K., and Gilbert, M. T. P. (2015). Tag jumps illuminated - reducing
588 sequence-to-sample misidentifications in metabarcoding studies. *Molecular Ecology Resources*,
589 15(6):1289–1303.

590 Shelton, A. O., O'Donnell, J. L., Samhouri, J. F., Lowell, N., Williams, G. D., and Kelly, R. P.
591 (2016). A framework for inferring biological communities from environmental DNA. *Ecological*
592 *Applications*, 26(6):1689–.

593 Shogren, A. J., Tank, J. L., Andruszkiewicz, E. A., Olds, B., Jerde, C., and Bolster, D. (2016).
594 Modelling the transport of environmental DNA through a porous substrate using continuous
595 flow-through column experiments. *Journal of The Royal Society Interface*, 13(119):423–425.

596 Simpson, E. H. (1949). Measurement of diversity. *Nature*, 163(688).

597 Spiess, A.-N. (2014). *propagate: Propagation of Uncertainty*.

598 Strathmann, M. F. (1987). *Reproduction and Development of Marine Invertebrates of the Northern*
599 *Pacific Coast: Data and Methods for the Study of Eggs, Embryos, and Larvae*. University of
600 Washington Press, Seattle.

601 Strathmann, M. F. and Strathmann, R. R. (2006). A Vermetid Gastropod with Complex Intracap-
602 sular Cannibalism of Nurse Eggs and Sibling Larvae and a High Potential for Invasion. *Pacific*
603 *Science*, 60(1):97–108.

604 Strickland, R. M. (1983). *The Fertile Fjord: Plankton in Puget Sound*. University of Washington
605 Press, Seattle.

606 Strickler, K. M., Fremier, A. K., and Goldberg, C. S. (2015). Quantifying effects of UV-B, temper-
607 ature, and pH on eDNA degradation in aquatic microcosms. *Biological Conservation*, 183:85–92.

608 Thomsen, P. F., Kielgast, J., Iversen, L. L., Møller, P. R., Rasmussen, M., and Willerslev, E. (2012).
609 Detection of a Diverse Marine Fish Fauna Using Environmental DNA from Seawater Samples.
610 *PLoS ONE*, 7(8):1–9.

611 Turner, C. R., Uy, K. L., and Everhart, R. C. (2015). Fish environmental DNA is more concentrated
612 in aquatic sediments than surface water. *Biological Conservation*, 183:93–102.

613 Tyson, G. W., Chapman, J., Hugenholtz, P., Allen, E. E., Ram, R. J., Richardson, P. M.,
 614 Solovyev, V. V., Rubin, E. M., Rokhsar, D. S., and Banfield, J. F. (2004). Community structure
 615 and metabolism through reconstruction of microbial genomes from the environment. *Nature*,
 616 428(6978):37–43.

617 Venter, J. C., Remington, K., Heidelberg, J. F., Halpern, A. L., Rusch, D., Eisen, J. a., Wu, D.,
 618 Paulsen, I., Nelson, K. E., Nelson, W., Fouts, D. E., Levy, S., Knap, A. H., Lomas, M. W.,
 619 Nealson, K., White, O., Peterson, J., Hoffman, J., Parsons, R., Baden-Tillson, H., Pfannkoch,
 620 C., Rogers, Y.-H., and Smith, H. O. (2004). Environmental genome shotgun sequencing of the
 621 Sargasso Sea. *Science*, 304(5667):66–74.

622 Wetzel, C. E., de Bicudo, D. C., Ector, L., Lobo, E. A., Soininen, J., Landeiro, V. L., and Bini,
 623 L. M. (2012). Distance Decay of Similarity in Neotropical Diatom Communities. *PLoS ONE*,
 624 7(9):e45071.

625 Yang, Z. and Khangaonkar, T. (2010). Multi-scale modeling of Puget Sound using an unstructured-
 626 grid coastal ocean model: From tide flats to estuaries and coastal waters. *Ocean Dynamics*,
 627 60(6):1621–1637.

628 Zhang, J., Kobert, K., Flouri, T., and Stamatakis, A. (2014). PEAR: A fast and accurate Illumina
 629 Paired-End reAd mergeR. *Bioinformatics*, 30(5):614–620.

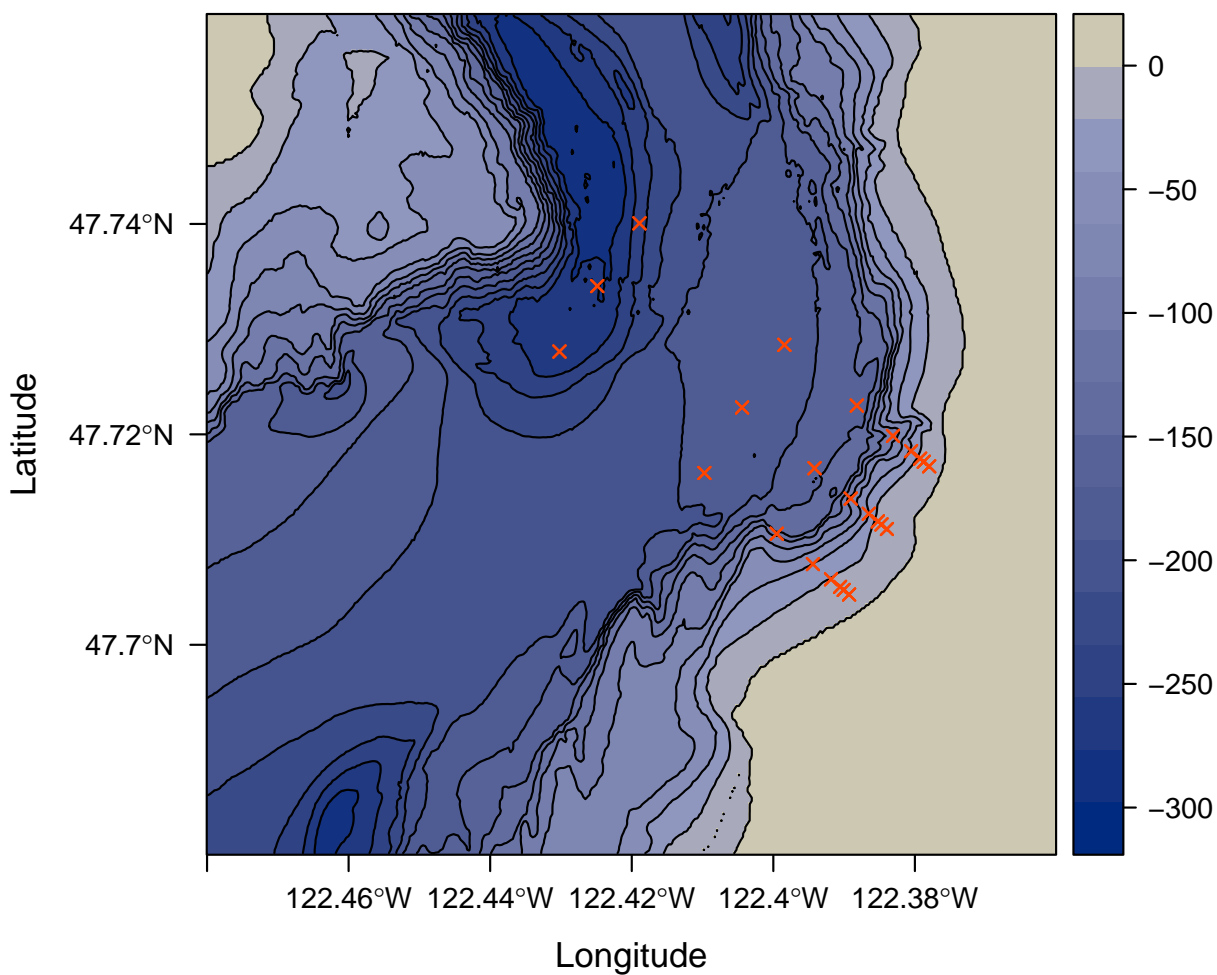


Figure 1: Map of study area. Depth in meters below sea level is indicated by shading and 25 meter contours. Sampled locations are indicated by red points.

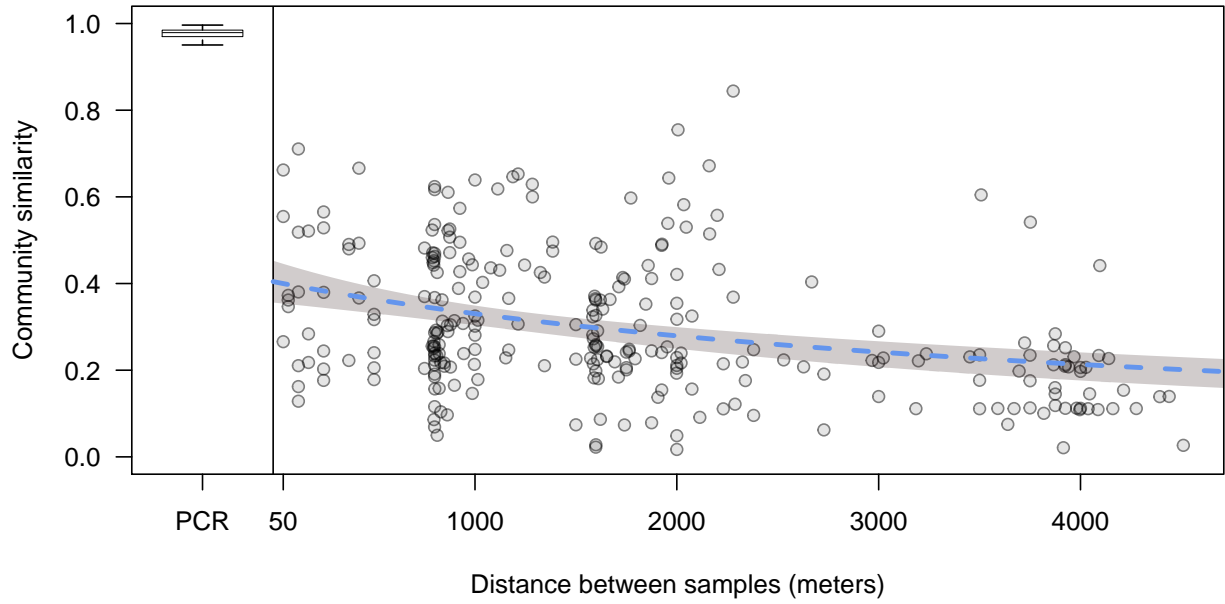


Figure 2: Distance decay relationship of environmental DNA communities. Each point represents the Bray-Curtis similarity of a site sampled along three parallel transects comprising a 3000 by 4000 meter grid. Blue dashed line represents fit of a nonlinear least squares regression (see Methods), and shading denotes the 95% confidence interval. Boxplot is comparisons within-sample across PCR replicates, separated by a vertical line at zero, where the central line is the median, the box encompasses the interquartile range, and the lines extend to 1.5 times the interquartile range. Boxplot outliers are omitted for clarity.



Figure 3: Cluster membership of sampled sites. Distance from onshore starting point is log scaled. Sites are colored and labeled by their assignment to a cluster by PAM analysis for number of clusters (K) chosen based on a priori expectations (2) and mean silhouette width (8).

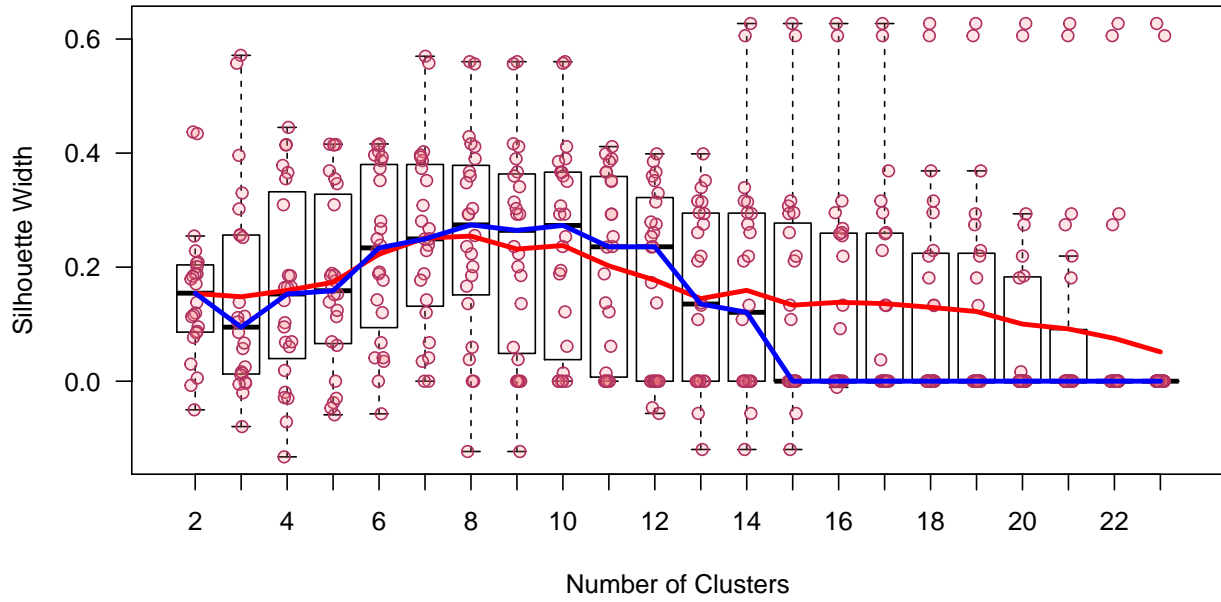


Figure 4: Silhouette widths from PAM analysis. Points are the width of the PAM silhouette of each sample at each number of clusters (K). Red line is the mean, blue line is the median. Boxes encompass the interquartile range with a line at the median, and the whiskers extend to 1.5 times the interquartile range. Boxplot outliers are omitted for clarity.



Figure 5: Aggregate measures of diversity at each sample site.

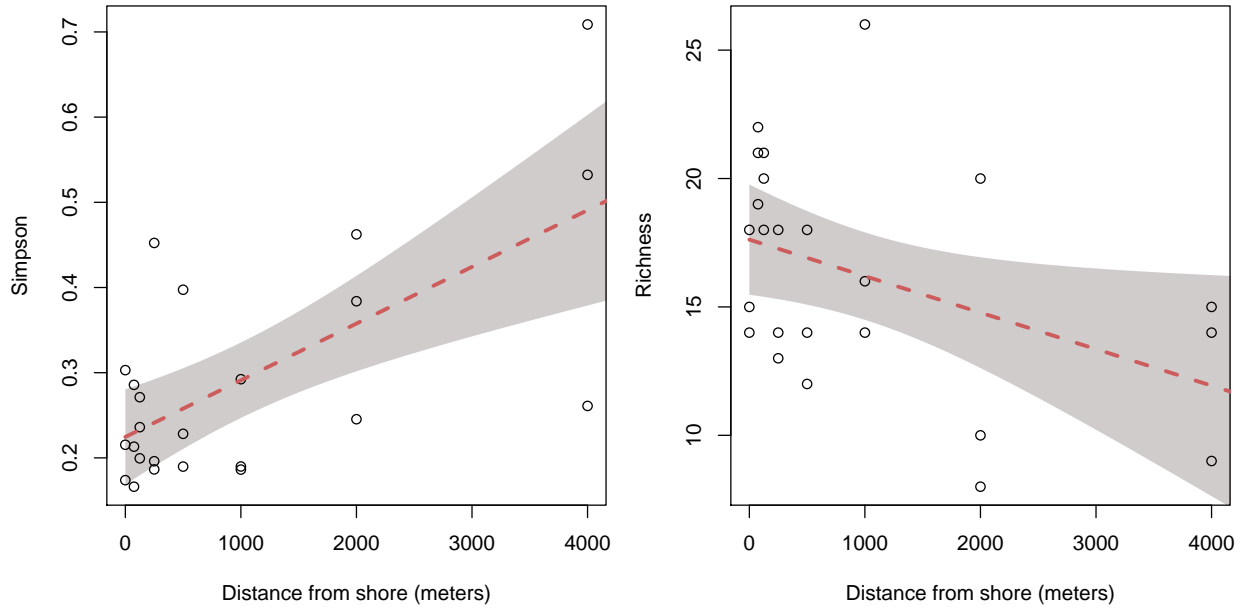


Figure 6: Aggregate diversity metrics of each site plotted against distance from shore. Both Simpson's Index (left) and richness (right) are shown, and have been computed from the mean abundance of unique DNA sequences found across 4 PCR replicates at each of 24 sites. Lines and bands illustrate the fit and 95

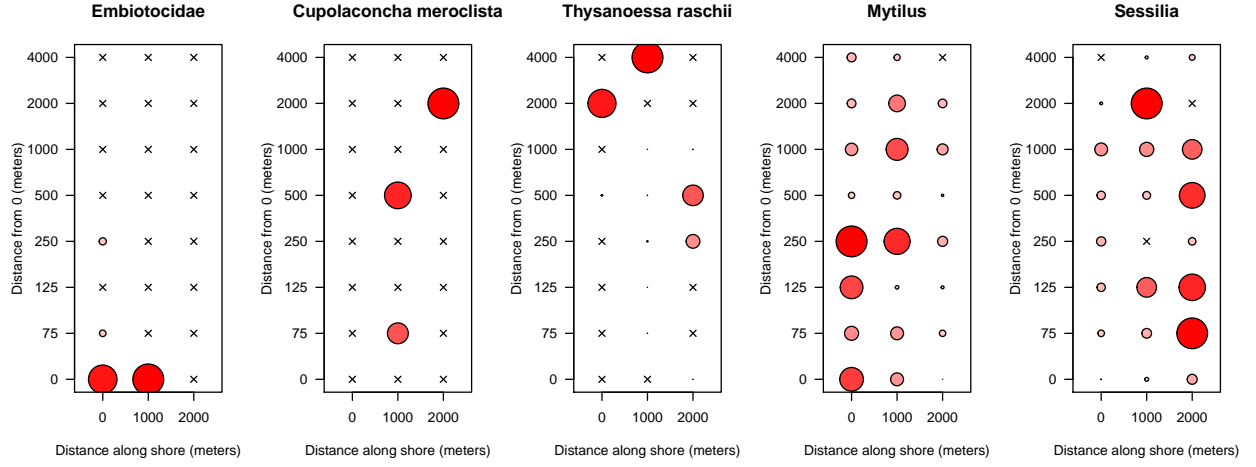


Figure 7: Distribution of eDNA from select taxa. Circles are colored and scaled by the proportion of that taxon's maximum proportional abundance. That is, the largest circle is the same size in each of the panels, and occurs where that taxon contributed the greatest proportional abundance of reads to that sample.

Supplemental Material

Methods

Bioinformatics

Reads passing the preliminary Illumina quality filter were demultiplexed on the basis of the adapter index sequence by the sequencing facility. We used fastqc to assess the fastq files output from the sequencer for low-quality indications of a problematic run. Forward and reverse reads were merged using PEAR v0.9.6 Zhang et al. (2014) and discarded if more than 0.01 of the bases were uncalled. If a read contained two consecutive base calls with quality scores less than 15 (i.e. probability of incorrect base call = 0.0316), these bases and all subsequent bases were removed from the read. Paired reads for which the probability of matching by chance alone exceeded 0.01 were not assembled and omitted from the analysis. Assembled reads were discarded if assembled sequences were not between 50 and 168 bp long, or if reads did not overlap by at least 100 bp.

We used vsearch v2.1.1 (Rognes et al., 2016) to discard any merged reads for which the sum of the per-base error probabilities was greater than 0.5 (“expected errors”) Edgar (2010). Sequences were demultiplexed on the basis of the primer index sequence at base positions 4-9 at both ends using the programming language AWK. Primer sequences were removed using cutadapt v1.7.1 Martin (2011), allowing for 2 mismatches in the primer sequence. Identical duplicate sequences were identified, counted, and removed in python to speed up subsequent steps by eliminating redundancy, and sequences occurring only once were removed. We checked for and removed any sequence likely to be a PCR artifact due to incomplete extension and subsequent mis-priming using a method described by Edgar (2010) and implemented in vsearch v2.0.2. Sequences were clustered into operational taxonomic units (OTUs) using the single-linkage clustering method implemented by swarm version 2.1.1 with a local clustering threshold (d) of 1 and fastidious processing (Mahé et al., 2014).

Cross-contamination of environmental, DNA, or PCR samples can result in erroneous inference about the presence of a given DNA sequence in a sample. However, other processes can contribute to the same signature of contamination. For example, errors during oligonucleotide synthesis or sequencing of the indexes could cause reads to be erroneously assigned to samples. The frequency of such errors can be estimated by counting the occurrence of sequences known to be absent from

659 a given sample, and of reads that do not contain primer index sequences in the expected position
660 or combinations. These occurrences indicate an error in the preparation or sequencing procedures.
661 We estimated a rate of incorrect sample assignment by calculating the maximum rate of occur-
662 rence of index sequences combinations we did not actually use, as well as the rates of cross-library
663 contamination by counting occurrences of primer sequences from 12S amplicons prepared in a lab
664 more than 1000 kilometers away, but pooled and sequenced alongside our samples. This represents
665 a general minimum rate at which we can expect that sequences from one environmental sample
666 could be erroneously assigned to another, and so we considered for further analysis only those reads
667 occurring with greater frequency than this across the entire dataset.

668 We checked for experimental error by evaluating the Bray-Curtis similarity (1 - Bray-Curtis
669 dissimilarity) among replicate PCRs from the same DNA sample. We calculated the mean and
670 standard deviation across the dataset, and excluded any PCR replicates for which the similarity
671 between itself and the other replicates was less than 1.5 standard deviations from the mean.

672 To account for variation in the number of sequencing reads (sequencing depth) recovered per
673 sample, we rarefied the within-sample abundance of each OTU by the minimum sequencing depth
674 (Oksanen et al., 2016).

675 Because each step in this workflow is sensitive to contamination, it is possible that some se-
676 quences are not truly derived from the environmental sample, and instead represent contamination
677 during field sampling, filtration, DNA extraction, PCR, fragment size selection, quantitation, se-
678 quencing adapter ligation, or the sequencing process itself. We take the view that contaminants
679 are unlikely to manifest as sequences in the final dataset in consistent abundance across replicates;
680 indeed, our data show that the process from PCR onward is remarkably consistent. Thus, after
681 scaling to correct for sequencing depth variation, we calculated from our data the maximum number
682 of sequence counts for which there is turnover in presence-absence among PCR replicates within an
683 environmental sample. We use this number to determine a conservative minimum threshold above
684 which we can be confident that counts are consistent among replicates and not of spurious origin,
685 and exclude from further analysis observations where the mean abundance across PCR replicates
686 within samples does not reach this threshold. For further analyses we use the mean abundance
687 across PCR replicates for each of the 24 environmental samples.

688 In order to determine the most likely taxon from which each sequence originated, the representa-

689 tive sequence from each OTU was then queried against the NCBI nucleotide collection (GenBank;
690 version October 7, 2015; 32,827,936 sequences) using the blastn command line utility (Camacho
691 et al., 2009). In order to maximize the accuracy of this computationally intensive step, we imple-
692 mented a nested approach whereby each sequence was first queried using strict parameters (e-value
693 = 5e-52), and if no match was found, the query was repeated with decreasingly strict e-values (5e-48
694 5e-44 5e-40 5e-36 5e-33 5e-29 5e-25 5e-21 5e-17 5e-13). Other parameters were unchanged among
695 repetitions (word size: 7; maximum matches: 1000; culling limit: 100; minimum percent identity:
696 0). Each query sequence can be an equally good match to multiple taxa either because of invariabil-
697 ity among taxa or errors in the database (e.g. human sequences are commonly attributed to other
698 organisms when they in fact represent lab contamination). In order to guard against these spurious
699 results, we used an algorithm to find the lowest common taxon for at least 80% of the matched
700 taxa, implemented in the R package taxize 0.7.8 (Chamberlain and Szöcs, 2013; Chamberlain et al.,
701 2016). Similarly, we repeated analyses using the dataset consolidated at the same taxonomic rank
702 across all queries, for the rank of both family and order.

703 **Alternative distance decay model formulations**

704 **Linear:** We fit a straight line through the points after log-transforming the spatial distances
705 to estimate the intercept and slope. This model ignores the bounds of our response variable of
706 community similarity.

707 **Michaelis-Menten:** We fit a Michaelis-Menten-like curve to our data. Our formulation can be
708 thought of as a modification of the Michaelis-Menten equation, but with the addition of a parameter
709 in the numerator which modifies the intercept.

$$y = \frac{AB + Cx}{B + x} \quad (2)$$

710 Where C is the asymptote of minimum similarity. This formulation allows us to estimate the
711 maximum similarity in the system, and the rate at which it is achieved. If the value of the parameter
712 (AB) is 0 (i.e. if the intercept is 0), the form is identical to the Michaelis-Menten equation:

$$y = \frac{Cx}{B+x} \quad (3)$$

713 This is conceptually satisfying in that a fit through $[0,1]$ reflects the theoretical expectation that
714 samples at zero distance from one another are necessarily identical. Given an efficient sampling
715 technique, replicate samples taken at the same position in space should be identical, and thus the
716 intercept of the regression of similarity against distance should be 1, and deviation from 1 is an
717 indicator of the efficiency of the sampling method.

718 Finally, we considered a model which estimates an asymptote as the total change in similarity
719 (D):

$$y = \frac{A + Dx}{B + x} \quad (4)$$

720 However, this model failed to converge and produced uninformative estimates of all parameters.

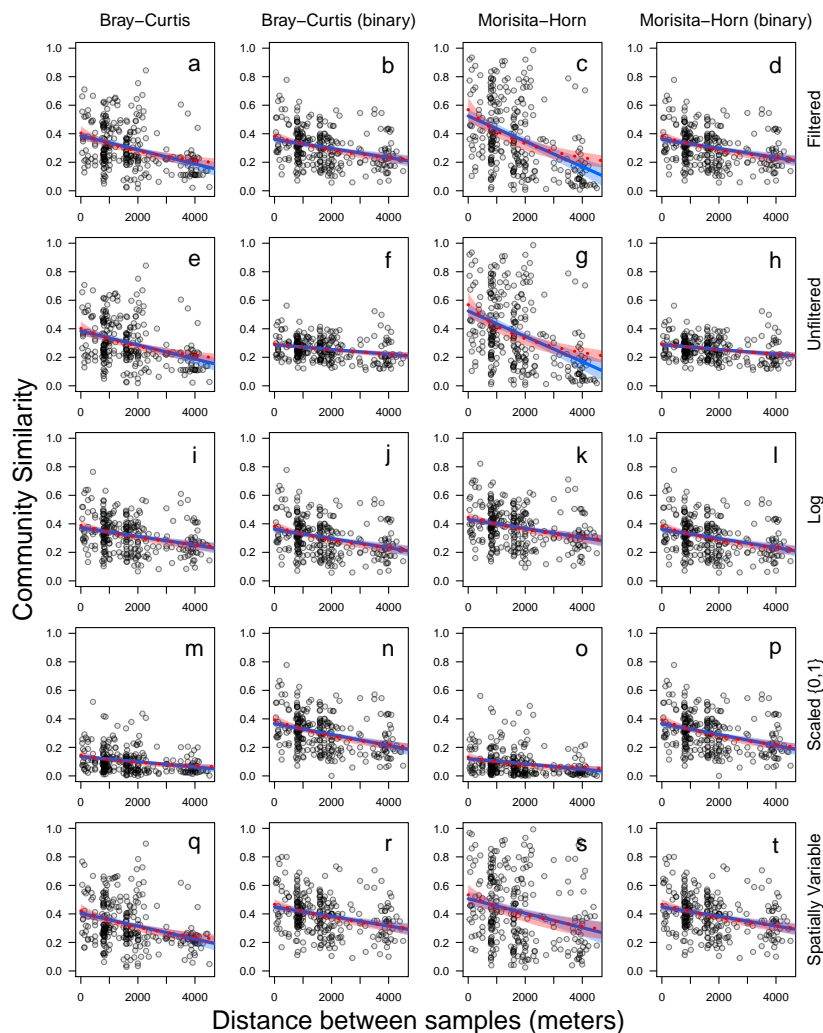


Figure 8: Distance decay relationship of environmental DNA communities using a variety of models, metrics, and data subsets. Each point represents the similarity of a site sampled along three parallel transects comprising a 3000 by 4000 meter grid. Each row of plots represents a different data subset indicated in the right margin, including the final filtered data reported in the main text (a-d), the unfiltered data including all rare OTUs (e-h), log-transformed ($\log(x+1)$) data (i-l), OTU abundance scaled relative to within-taxon maximum (m-p), and exclusion of OTUs found at only one site (q-t). Columns indicate the similarity index used (Bray Curtis or Morisita-Horn) and whether the input was full abundance data or binary (0,1) transformed data. Lines and bands illustrate the fit and 95% confidence interval of both the main nonlinear model (red, dashed line) and a simple linear model (blue, solid line). Results using the Jaccard distance are omitted because of its similarity to Bray-Curtis.

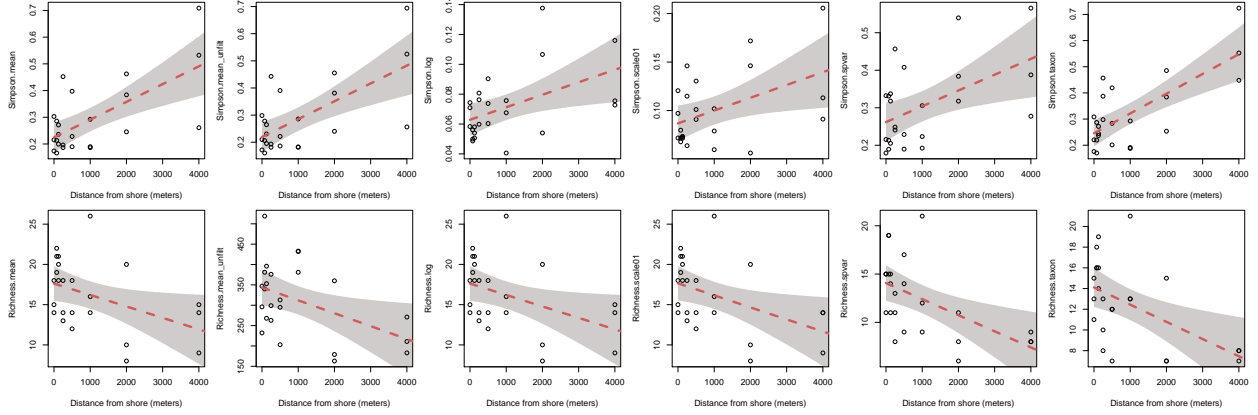


Figure 9: Aggregate diversity metrics of each site plotted against distance from shore. Both Simpson's Index (top) and richness (bottom) are shown for a variety of data subsets and transformations (left to right: mean, unfiltered mean, $\log(x + 1)$, transformed, scaled, spatially variable, and taxon clustered). Lines and bands illustrate the fit and 95% confidence interval of a linear model. See methods text for detailed data descriptions.